

Preparation and characterization of mullite tubular membranes

Omid Bakhtiari, Mohammad Samei, Hamid Taghikarimi, Toraj Mohammadi*

Research Center for Membrane Separation Processes, Department of Chemical Engineering, Iran University of Science and Technology (IUST), Narmak, Tehran, Iran. Tel./fax: +982177240051; email: torajmohammadi@iust.ac.ir

Received 10 November 2010; accepted 1 March 2011

ABSTRACT

Sintering of tubular extruded kaolin as microfilter membranes was investigated. Design of Experiments was carried out using Taguchi method. Effects of sintering temperature (1,150, 1,225 and 1,300°C) and time (1, 3 and 5 h), calcination temperatures of 550 (0, 2 and 4 h) and 950°C (1, 3 and 5 h) with heating rate of 2°C/min were studied. XRD and mercury porosimetry analysis were performed to characterize the membranes. Different characteristics including mechanical strength, weight loss, linear and cross shrinkage, and water permeation were also studied. Membranes were found to have good properties as microfilters and/or supports for different zeolite membranes.

Keywords: Mullite; Tubular membrane; Microfilter; Sintering; Membrane properties

1. Introduction

Membrane based separation technology, as green and environmentally friendly technology is a fast growing branch of science and engineering and has found a widespread usage in biotechnological, pharmaceutical, food industries. Treatment of different industrial effluents since continuous operation is possible in these processes and they could be hybridized easily with other separation processes [1-5]. Many worldwide researches are working in the improvement or renewal of current membrane processes and materials. Membrane materials range from polymeric to minerals (ceramics, metals and glasses) in different modular forms. Each of them present advantages and disadvantages including low cost and good processability for polymeric and high mechanical and thermal strengths and corrosive resistance in acid and base media with nearly uniform pore size distribution for inorganic membranes. Disadvantages include non-

uniform pore size distribution, operating temperature limit and tradeoff between permeability and selectivity for polymeric membranes and low specific surface area in module and high cost for ceramic membranes [2-5].

Ceramic membranes are used instead of polymeric membranes in a number of industrial fields because of their outstanding chemical, thermal and mechanical strength where more expensive cost for ceramic membranes than polymeric membranes is compensated by these superior properties. In addition, pore size in these membranes can be better controlled and as a consequence their pore size distribution is generally very narrow. Their long life and good antifouling, ion exchange and catalytic properties should be added to these superior properties. Various techniques can be used to prepare ceramic membranes, being sintering, sol/gel process, anodic oxidation, extrusion, centrifugal deposition, press molding and isostatic pressing the main ones [1-10].

Ceramic tubular membranes are usual in application because of their higher flux at higher separation

*Corresponding author

Table 1
Kaolin (named SZWNL1) composition as reported by the manufacturer, Iran China Clay Industries Company

Component name	SiO ₂	Al ₂ O ₃	Fe ₂ O ₃	TiO ₂	CaO	MgO	Na ₂ O	K ₂ O	L.O.I
Mole %	63.63	24.05	0.65	0.04	1.40	0.50	0.30	0.20	9.22

factors [3,11]. There are many applications for tubular porous membranes ranging from microfilters (MF) and/or ultrafilters (UF) as supports for zeolite and/or hybrid membranes due to their wide but nearly uniform distribution of pore sizes, other than those of mesoporous inorganic membranes made them suitable even though for narrow size distributed emulsions of W/O or O/W [3,6,12]. Many research works were carried out on manufacturing of these types of membranes but authors of this work followed the approach of investigation of synthesis parameters like calcination and sintering temperatures and times on membrane properties including porosity, water permeation flux, mechanical strength, weight loss and linear shrinkage.

There are many characterization techniques evaluating ceramic membrane structure and specifications like mean pore size and complete pore size distribution (PSD), frequently obtained from N₂ adsorption/desorption experiments, bubble point equipment and mercury porosimetry. Other information can be obtained from measurements of water/liquid or gas permeability, SEM, XRD, and so on. It seems clear that all techniques can be considered as not excluding the others, because all of them can give important complementary information whose comparison and proper analysis reveal a complete picture of the studied membrane [2,4,13].

Considering separation, mechanical strength is needed to endure aggressive environment including pressure difference across the membrane or stresses which the ceramic components are subjected to (residual stresses), differential thermal expansion coefficient, temperature gradient, and/or external mechanical loading or pressure fluctuation in the process. Magnitudes of the stresses depend on the material properties, the operating conditions and the geometry of design [3,14].

Clay minerals are a well-known cheap class of natural inorganic materials, with well-known structural adsorption, rheological and thermal properties [5,15]. As sintering of these materials proceed, they experience weight loss weights are loss to some extent. Weight loss is evidence of some reactions like dehydroxylation when kaolin temperature raises and meta-kaolin and mullite is formed [11,16].

In this study, tubular extruded kaolin was sintered and porous membranes were prepared using kaolin with composition reported in Table 1 [17]. Analysis including water absorption, water permeation flux, dimension measurement, mechanical strength, and weight loss of sintered membranes were performed. XRD and mercury porosimetry analysis were also used to characterize the membranes.

2. Experiments

Micronized China clay was suspended in distilled water using Stuart stirrer (SS20) and then filtered using a 400 mesh sieve (Damavand test sieves Ltd., particle size < 37 μm). The suspension was allowed to settle inside its container and the upper clear water was removed periodically. Finally, a homogeneous mud was obtained after around a week. Tubular membranes were then extruded using aged uniformed mud with length, outer and inner diameter of 170, 14.3, and 9.3 mm, respectively. For uniform drying and to avoid mechanical stress when tubes were dried, wet extrudates were placed inside an oven at 100°C for a few hours. After that the dried extrudates were placed inside a furnace (Zohouri Furnace Industries) at different calcination and sintering temperatures and for different times, with a heating rate of 2°C/min.) Based on thermal analysis (Fig. 1, TGA and DTA analysis were carried out at atmosphere of Ar and heating rate of 10°C/min using PL-SPA1500 apparatus) different calcination times at 550°C and 950°C were applied. As

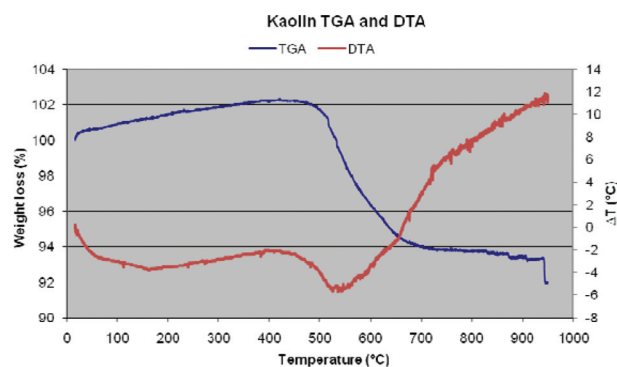


Fig. 1. TGA and DTA of kaolin sample used in the experiments.

Table 2
Preliminary study of effective parameters based on the Taguchi method

Sintering temperature (°C)	Time (h)	Heating rate (°C/h)	Calcination time at 600°C (h)
1,000	1	1	0
1,000	2	2	2
1,000	3	3	4
1,100	1	2	4
1,100	2	3	0
1,100	3	1	2
1,200	1	3	2
1,200	2	1	4
1,200	3	2	0

observed, weight loss of calcination starts at evaluated temperatures upper than 500–550°C. 950°C is the maximum temperature as reported in TGA analysis. In order to save time and money, Taguchi method of Design of Experiments was employed. Some preliminary studies based on Table 2 (not all of them) were carried out to evaluate the importance of different parameters. The results showed that sintering temperature and time have the most important effect on different properties of the membranes under investigation. However, sintered membranes at 1,000 and 1,100°C had not enough mechanical strength and their color was pink instead of white. As result, sintering temperature was increased as reported in Table 3. Based on the results, effect of heating rate in the studied properties was not significant and thus excluded from the studied parameters, and average heating rate of 2°C/min was used for all the experiments [18,19]. Finally different parameters of each sintering run are reported in Table 3 (L9 array in Taguchi method where four parameters with three different levels for each are considered) [20].

XRD patterns were recorded using a Philips 1480 diffractometer using Cu-K α radiation (θ –2 θ , 40 kV and 30 mA). Mercury porosimetry was performed using Pascal 440 (one normal dilatometer with maximum pressure of 400 bar).

After sintering, different properties of the membranes like porosity, dead end distilled water flux at applied pressure of 3 bar for 3 min, mechanical strength, weight loss, and linear shrinkage were evaluated. In order to determine the membrane porosity, sintered membranes were dried at 120°C for 3 h and weighted. Then they were placed in distilled water overnight and then weighted again. Knowing dry (W_0) and wet (W_W) weights of the membranes and their total volumes, porosity was calculated according to the following equation:

Table 3
Different parameters of sintering runs based on the Taguchi method

Sintering temperature (°C)	Sintering time (h)	Calcination time at 550°C (h)	Calcination time at 950°C (h)
1,150	1	0	1
1,150	3	2	3
1,150	5	4	5
1,225	1	2	5
1,225	3	4	1
1,225	5	0	3
1,300	1	4	3
1,300	3	0	5
1,300	5	2	1

$$\text{Porosity Percent} = \frac{W_W - W_0}{\rho_W V_M} * 100, \quad (1)$$

where ρ_W and V_M stand for water density (25°C) and membrane volume, respectively.

Mechanical strength of the prepared membranes was evaluated using a hydraulic jack (Fig. 2). They were pressed in a direction perpendicular to their axis and the rupture pressure was recorded as an index of the membrane mechanical strength.

Dead end distilled water flux was measured using an apparatus schematically represented in Fig. 3. When steady state permeation of distilled water was attained, permeated distilled water was collected during 3 min at 3 bar pressure difference across the membrane, and weighted (P_w). Distilled water flux was calculated using the following formula:

$$F = \frac{P_w}{\pi OD_M L_M t}, \quad (2)$$

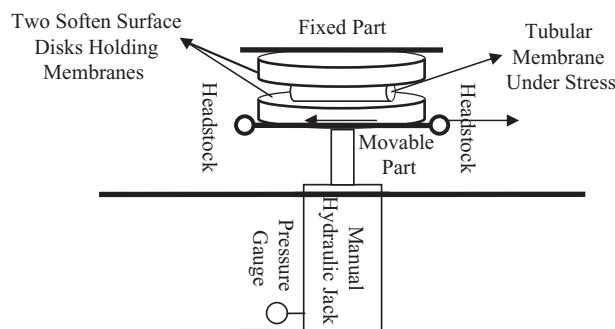


Fig. 2. Schematic diagram of hydraulic jack used in evaluating mechanical strengths of the manufactured membranes.

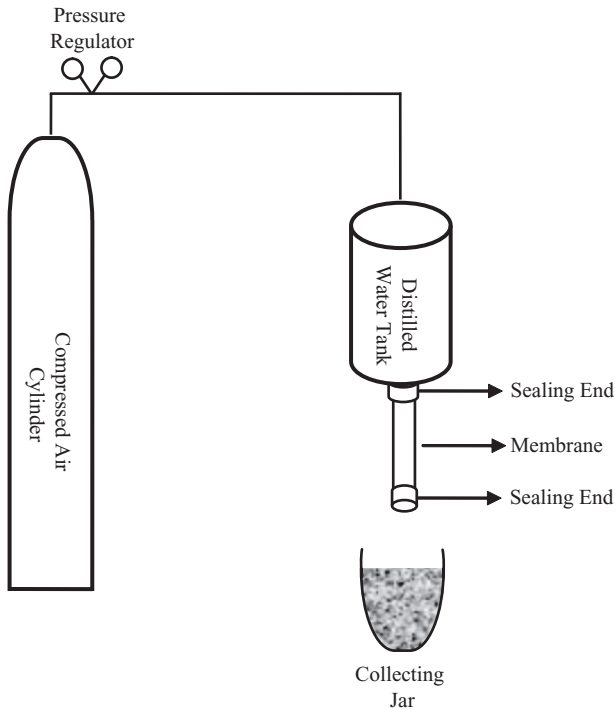


Fig. 3. Schematic diagram of apparatus used in distilled water permeation measurement of the manufactured membranes.

where F is flux, OD_M and L_M are membrane outer diameter and length, respectively, and t stands for permeation time.

Weight loss and linear and cross shrinkages of the sintered membranes were calculated with respect to raw extrudates weight and dimensions using the following formulas:

$$\text{Weight Loss} = \frac{W_W - W_S}{W_R} * 100, \tag{3}$$

$$\text{Linear Shrinkage} = \frac{L_R - L_S}{L_R} * 100, \tag{4}$$

$$\text{Cross Shrinkage} = \frac{OD_R - OD_S}{OD_R} * 100, \tag{5}$$

where W_R , L_R , and OD_R are weight, length, and outer diameter of raw extrudates, respectively and W_S , L_S , and OD_S are those of the sintered membrane.

3. Results and discussion

3.1. Porosity percent

As expected, sintered membranes densification occurs. Based on Rhines' topological decay model,

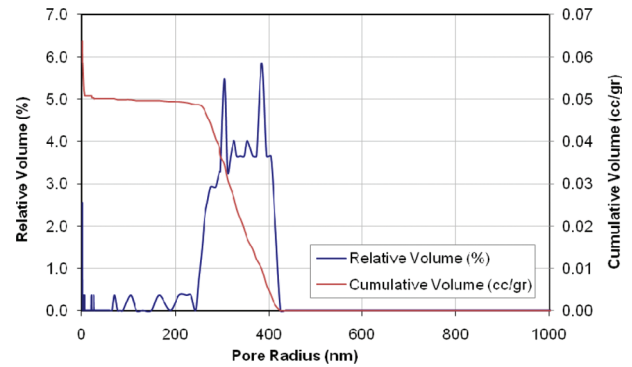


Fig. 4. Mercury porosimetry analysis of sintered membrane at 1,150°C for 3 h.

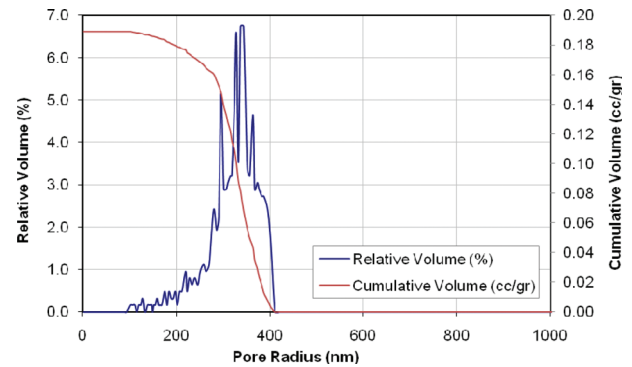


Fig. 5. Mercury porosimetry analysis of sintered membrane at 1,225°C for 3 h.

densification occurs in compensating length reduction and total channels number reduction inside the porous material [21]. While Rhines' model states pore diameter remained nearly constant as sintering temperature increases, mercury porosimetry analysis showed that pore radiuses of sintered membranes were increased with sintering temperature as shown in Figs. 4–6. Main pore size of sintered membrane versus sintering temperature is shown in Fig. 7. Results of Taguchi ANOVA analysis indicated that sintering temperature and time have the main effects on the membrane porosity. As it is shown, porosity decreases with increasing sintering temperature and time. In this case, pore number reduction compensates the pore radius (volumes) increment and the net effect is porosity reduction. Sintering temperature is 81.9% effective on the membrane porosity and sintering time is 7.1%. Effects of sintering temperature and time on membrane porosity are shown in Figs. 8 and 9, respectively. Other factors, as calcination time at 550 and 950°C have negligible effects on membrane porosity, since their F factors are less than 4.78 (for 95% certainty of effectiveness on the membrane porosity) [20]. Similar behavior of

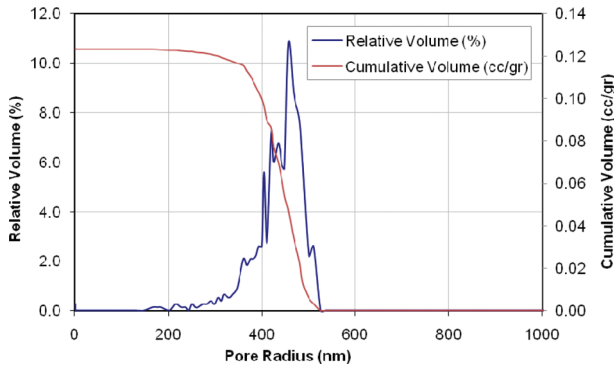


Fig. 6. Mercury porosimetry analysis of sintered membrane at 1,300°C for 3 h.

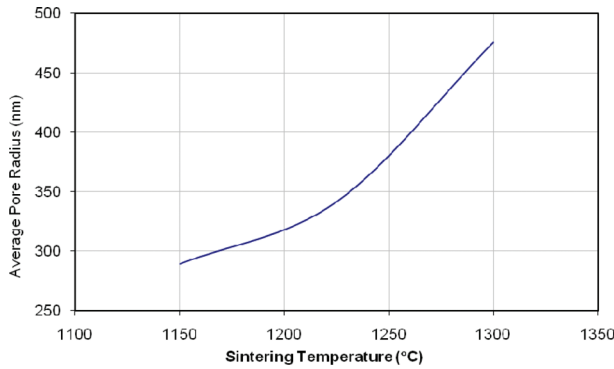


Fig. 7. Average membrane pore radius vs. sintering temperature.

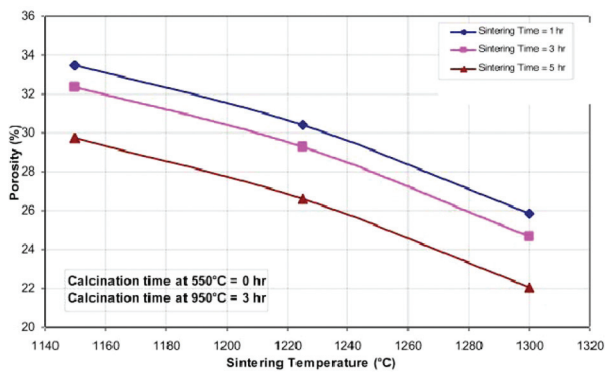


Fig. 8. Porosity of the sintered membranes as function of sintering temperature.

porosity variation with sintering temperature was reported by Bissett et al. [3].

Sintering heating rate is also another important factor affecting the membrane structure. But our rough characterization technique of water absorption was not able to detect this parameter effect on membrane structure. Finally it must be mentioned that deviation of the reported parameters from 100% can be attributed to

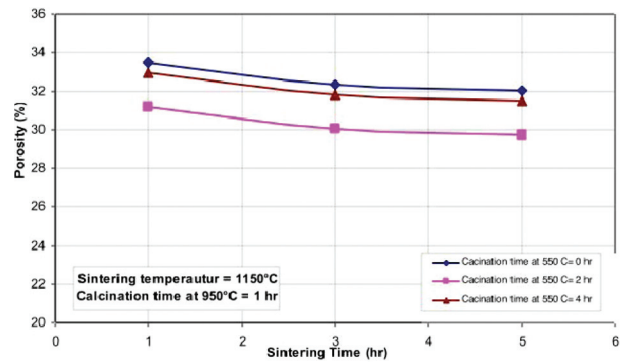


Fig. 9. Porosity of the sintered membranes as a function of sintering time.

this factor and other out of hand parameters like human and instrument errors.

3.2. Distilled water flux

As mentioned above, as porosity decreases with increasing sintering temperature and time, water permeation through the membranes is also expected to decrease. The results based on the Taguchi method, confirmed this expectation. This observation can be explained via Poiseuille equation [21]:

$$f = \frac{\pi \Delta P r^4}{8 \mu L}, \tag{6}$$

where f is a factor proportional to permeation flux of the membrane, ΔP is pressure difference across the membrane, r is pore radius, μ is flowing fluid viscosity and L is pore length. As observed, this equation includes three parameters involved in membrane flux: pore size and length and pore numbers (porosity). While pore radius is increasing for the synthesized membranes with sintering temperature, their length is slightly shorten, but their number (the membrane porosity) is reduced with increasing sintering temperature and as a result of the overall impact, water permeation flux decreases. The results showed that sintering temperature and time have the most important effects on permeation flux, 89 and 6%, respectively [20]. Calcination times at temperatures of 550 and 950°C have no significant effects on membrane flux (porosity). Permeation flux as function of sintering temperature and time are shown in Figs. 10 and 11, respectively.

3.3. Mechanical strength

Mechanical strength of sintered membranes was recorded according to the procedure above mentioned. According to the Taguchi method, sintering temperature

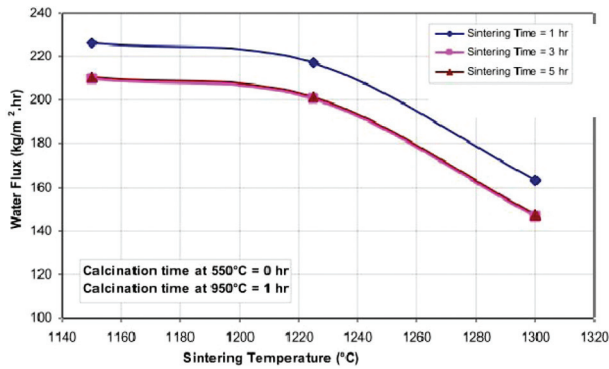


Fig. 10. Permeation water flux of the sintered membranes as a function of sintering temperature.

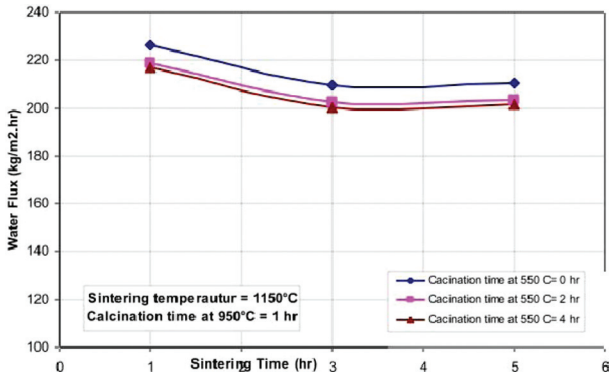


Fig. 11. Permeation water flux of the sintered as a function of sintering time.

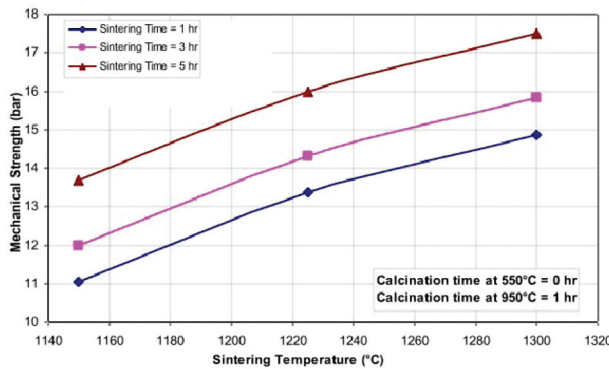


Fig. 12. Mechanical strength of sintered membrane as a function of sintering temperature.

and time have the most significant effect on mechanical strength of the membrane. Mechanical strength of the sintered membranes as function of sintering temperature and time are shown in Figs. 12 and 13, respectively. According to the Taguchi method, the contributions of sintering temperature and time on the membrane mechanical strength are respectively of 67% and 32%

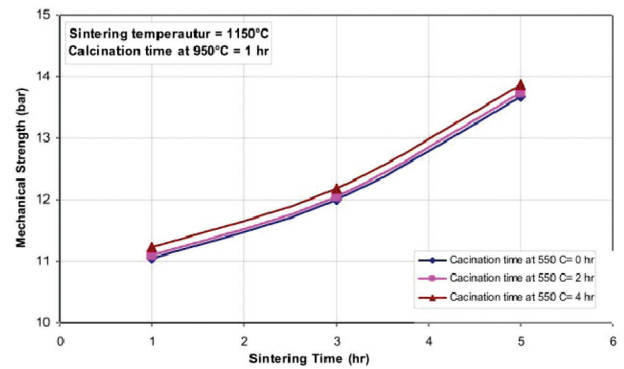
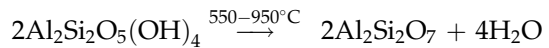


Fig. 13. Mechanical strength of sintered membrane as a function of sintering time.

[20]. Calcination times at 550 and 950°C have negligible effects on the mechanical strength of the membranes. The trend of mechanical strength variation with sintering temperature is in agreement with the results reported by Bissett et al. [3]. As Rhines' topological decay model states, shorter and less channels in number result in denser and tougher structure with higher mechanical strength for longer sintering time and at higher sintering temperature [21,22].

3.4. Weight loss

As calcination proceeds, some reactions such as dehydroxylation at temperatures around 550–950°C occur and poorly crystalline metakaolin is formed [16,23]:



This endothermic reaction can be followed in DTA analysis, as shown in Fig. 1 where required heat is increased as temperature increases from 500°C. As TGA analysis shows, the mass reductions at 650, 750, 850 and 945°C are 4.1%, 5.0%, 5.1% and 6.9% compared to that at 550°C, respectively. The mass reduction caused mainly by the evaporation of the structural water. Since all selected sintering temperatures were above calcination temperature of 950°C, i.e. >1,150°C where metakaolin is changed to mullite [23], exiting effects of volatile compounds and inert mass on weight loss could not be detected. XRD of sintered membranes are shown in Figs. 18–20). As observed, measured weight losses ranged from 9.2% to 10.6% (Eq. (3) was applied to calculate weight losses of all sintered membranes at different conditions as reported in Table 3) and this range was not wide enough to be analyzed with the Taguchi method. This range is wider than that obtained by TGA, and deviation is attributed to completion of dehydroxylation

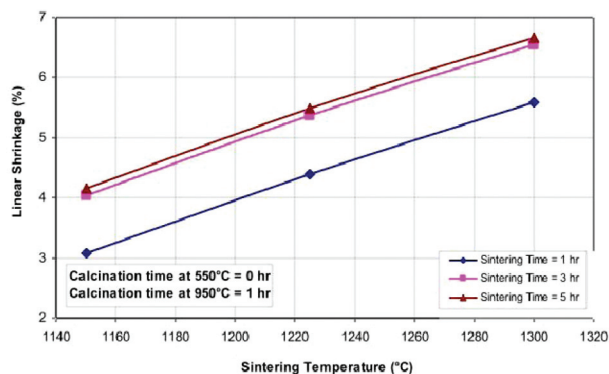


Fig. 14. Linear shrinkage of sintered membrane as a function of sintering temperature.

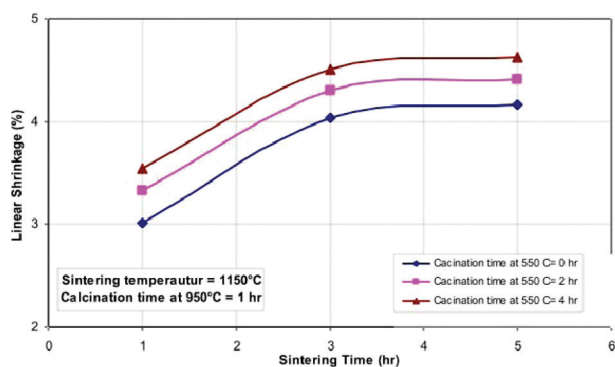


Fig. 15. Linear shrinkage of sintered membrane as a function of sintering time.

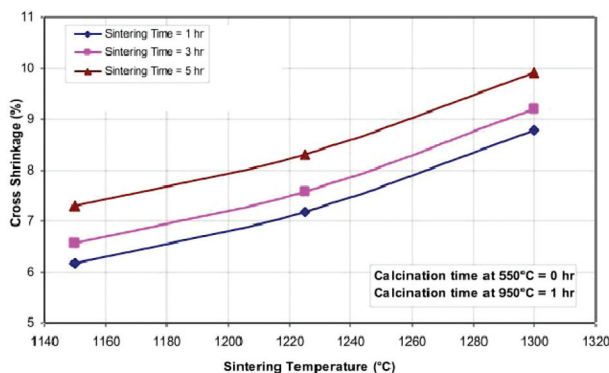


Fig. 16. Cross shrinkage of sintered membrane as a function of sintering temperature.

reaction occurring in the range of 950–1,050°C and longer sintering times (1–5 h and lower heating rate of 2°C/min) regarding to TGA (10°C/min) [23].

3.5. Linear and cross shrinkage

Linear and cross shrinkage of the sintered membrane were also studied. As the rest of the investigated

Table 4

F values for sintering time and temperature effects on different under investigation properties [14]

Property	Sintering temperature (°C)	Sintering time (h)
Porosity percent	98.3	9.4
Distilled water flux	368.32	27.6
Mechanical strength	1050.9	505.4
Weight loss	–	–
Linear shrinkage	59.0	13.2
Cross shrinkage	1056.5	198.5

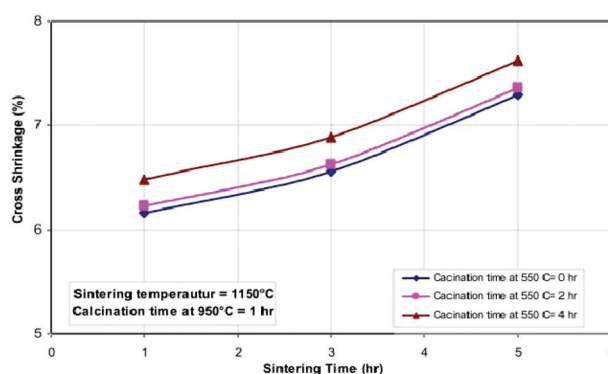


Fig. 17. Cross shrinkage of sintered membrane as a function of sintering time.

properties, linear and cross shrinkage were also affected by sintering temperature and time. Effect of sintering temperature and time on linear and cross shrinkage of the membranes, was analyzed using the Taguchi method and the results are shown in Figs. 14 and 15 for linear shrinkage and Figs. 15 and 16 for cross shrinkage [20]. Sintering temperature have 73% and 82% contribution on linear and cross shrinkage of membranes, respectively. Fewer contributions of 15% and 16% were observed for effects of sintering time on linear and cross shrinkage, respectively [20]. The results are in agreement with those reported by Bissett et al. [3].

F values of sintering temperatures and times for different properties, calculated by Taguchi method, are reported in Table 4 [20]. *F* values of greater than 3.24 show their corresponding variables are affecting parameters on selected membrane properties [20].

3.6. Complementary analyses

Some membranes were also analyzed with XRD and mercury porosimetry analysis. The XRD results are shown in Figs. 18–20. The major phases are Mullite (Al₆Si₂O₁₃), Cristobalite and Quartz (SiO₂). Cristobalite

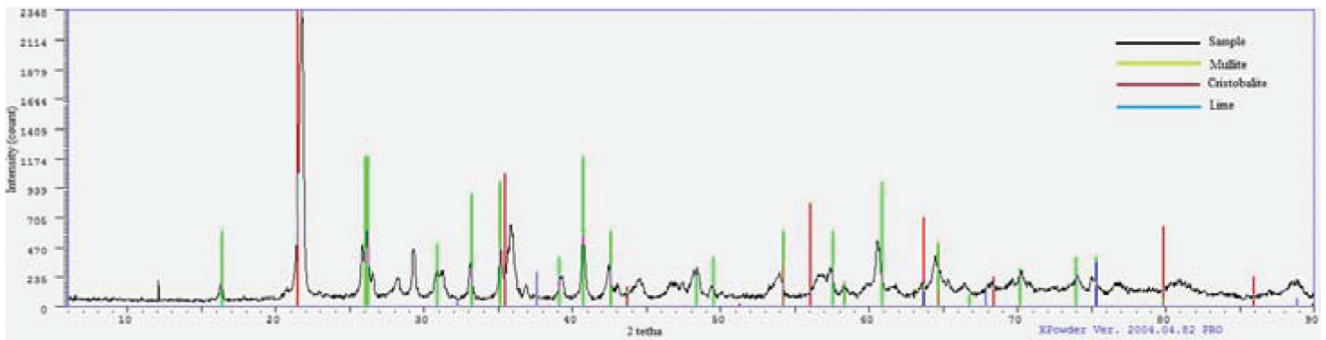


Fig. 18. XRD image of sintered membrane at 1,150°C for 3 h, major phases are Mullite ($\text{Al}_6\text{Si}_2\text{O}_{13}$) and Cristobalite (SiO_2), minor phases are Lime (CaO).

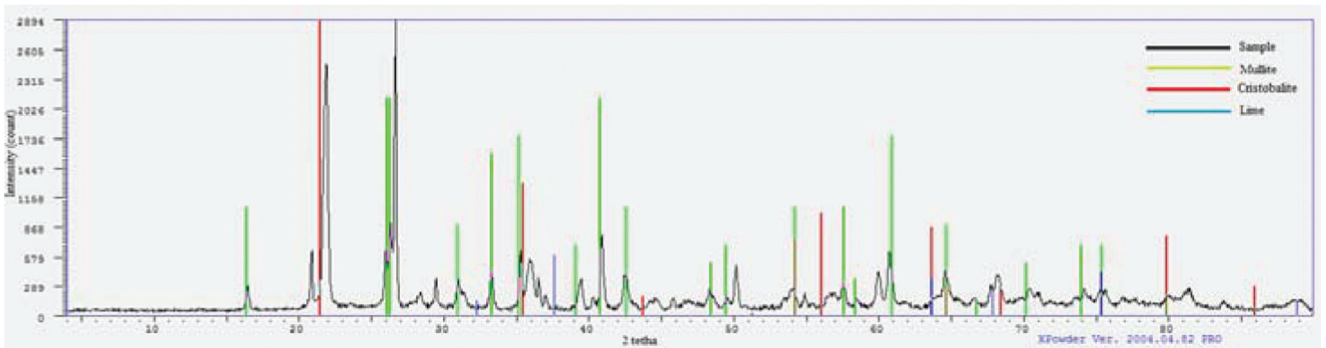


Fig. 19. XRD image of sintered membrane at 1,225°C for 3 h, major phases are Mullite ($\text{Al}_6\text{Si}_2\text{O}_{13}$), Cristobalite (SiO_2) and minor phase is Lime (CaO).

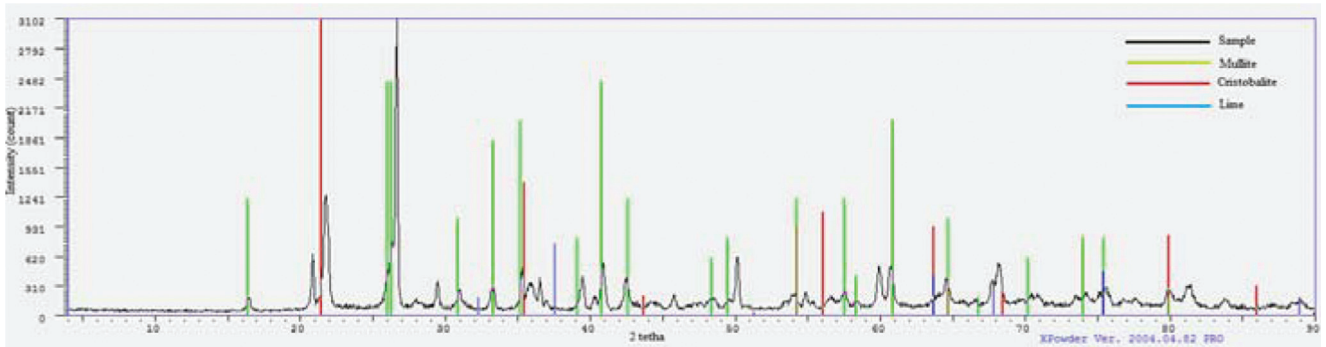


Fig. 20. XRD image of sintered membrane at 1,300°C for 3 h, major phases are Mullite ($\text{Al}_6\text{Si}_2\text{O}_{13}$), Cristobalite (SiO_2) and minor phase is Lime (CaO).

and Quartz could be removed by caustic soda washing (15% aqueous caustic soda, at 80°C for 5 h) and more open membrane structures could be obtained if needed [23]. Considering the XRD pattern of kaolin and metkaolin as shown in Fig. 21 [24], all XRD patterns of sintered membranes at different temperatures confirm mullite formation.

Porosimetry analysis was also carried out on those three sintered membranes studied by XRD. Volume

derivation with respect to pore radius is shown in Fig. 22. Results are in agreement with those reported by Wang et al. [21].

4. Conclusion

Tubular kaolin membranes were prepared and their properties were studied under different calcination and sintering temperatures and times. Sintering

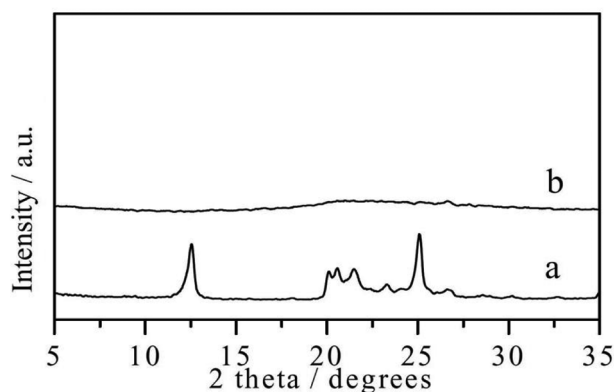


Fig. 21. XRD patterns of the kaolin (a) and metakaolin (b) [24].

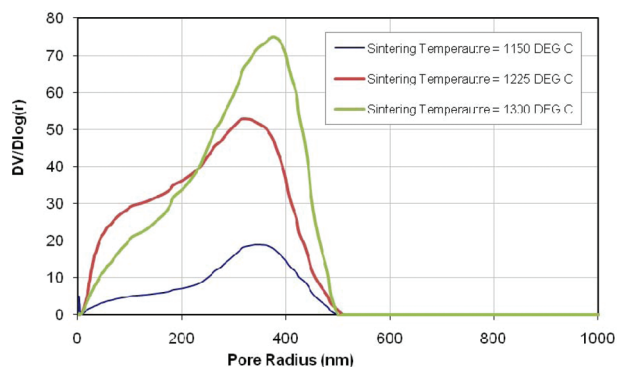


Fig. 22. Membrane pore derivation vs. PSD of sintered membrane.

temperature and time were found to have the most determinant effects on porosity percent, distilled water flux, mechanical strength, weight loss, linear and cross shrinkage of the sintered membranes. Prepared membranes have good properties to serve as supports for different zeolites for pervaporation and gas separation applications and also as microfilters in the case of free Cristobalite and Quartz (SiO_2) removal by washing with aqueous caustic soda for waste water treatment. Calcination time and temperature, $\text{SiO}_2/\text{Al}_2\text{O}_3$ ratio in kaolin samples, and also kaolin powder PSD effects are being on under investigation.

Acknowledgment

The financial support of Iranian national elite foundation and dedication different type of kaolin by Iran China Clay Industries Company are appreciated warmly.

References

- [1] T. Mohammadi et al., Experimental design in mullite microfilter preparation, *Desalination*, 184(1–3) (2005) 57–64.

- [2] Y. Dong et al., Fabrication and characterization of low cost tubular mineral-based ceramic membranes for micro-filtration from natural zeolite, *J. Membr. Sci.*, 281(1–2) (2006) 592–599.
- [3] H. Bissett, J. Zah and H.M. Krieg, Manufacture and optimization of tubular ceramic membrane supports, *Powder Technol.*, 181 (1) (2008) 57–66.
- [4] J.I. Calvo et al., Pore size distribution of ceramic UF membranes by liquid-liquid displacement porosimetry, *J. Membr. Sci.*, 310 (1–2) (2008) 531–538.
- [5] S. Khemakhem, R. Ben Amar and A. Larbot, Synthesis and characterization of a new inorganic ultrafiltration membrane composed entirely of Tunisian natural illite clay, *Desalination*, 206 (1–3) (2007) 210–214.
- [6] C. Liu et al., Synthesis and characterization of a mesoporous silica (MCM-48) membrane on a large-pore $\alpha\text{-Al}_2\text{O}_3$ ceramic tube, *Micropor. Mesopor. Mater.*, 106 (1–3) (2007) 35–39.
- [7] L.P. Jens Weitkamp, *Catalysis and Zeolites: Fundamentals and Applications*, Springer-Verlag, Berlin, Heidelberg, 1999.
- [8] Y. Dong et al., Reaction-sintered porous mineral-based mullite ceramic membrane supports made from recycled materials, *J. Hazard. Mater.*, 172 (1) (2009) 180–186.
- [9] Y.-Y. Chen and W.-C.J. Wei, Formation of mullite thin film via a sol-gel process with polyvinylpyrrolidone additive, *J. Eur. Ceram. Soc.*, 21 (14) (2001) 2535–2540.
- [10] G. Chen et al., Direct preparation of macroporous mullite supports for membranes by in situ reaction sintering, *J. Membr. Sci.*, 318 (1–2) (2008) 38–44.
- [11] Y. Dong et al., Cost-effective macro-porous mullite-corundum ceramic membrane supports derived from the industrial grade powder, *J. Alloys Compd.*, 477 (1–2) (2009) 350–356.
- [12] J. Wu et al., Preparation of W/O emulsions by membrane emulsification with a mullite ceramic membrane, *Desalination*, 193 (1–3) (2006) 381–386.
- [13] J.I. Calvo et al., Comparison of liquid-liquid displacement porosimetry and scanning electron microscopy image analysis to characterise ultrafiltration track-etched membranes, *J. Membr. Sci.*, 239 (2) (2004) 189–197.
- [14] P. Maarten Biesheuvel and H. Verweij, Design of ceramic membrane supports: permeability, tensile strength and stress, *J. Membr. Sci.*, 156 (1) (1999) 141–152.
- [15] Y.-F. Liu et al., Porous mullite ceramics from national clay produced by gelcasting, *Ceram. Int.*, 27 (1) (2001) 1–7.
- [16] Z. Zuhua et al., Role of water in the synthesis of calcined kaolin-based geopolymer, *Appl. Clay Sci.*, 43 (2) (2009) 218–223.
- [17] Product analysis report. 2009 Iran China Clay Industries Company.
- [18] R.M. de Vos and H. Verweij, Improved performance of silica membranes for gas separation, *J. Membr. Sci.*, 143 (1–2) (1998) 37–51.
- [19] Z. Ismagilov et al., Porous alumina as a support for catalysts and membranes. Preparation and study, *React. Kinet. Catal. Lett.*, 60 (2) (1997) 225–231.
- [20] D.C. Montgomery, *Design and Analysis of Experiments*, 3rd ed., John Wiley and Sons Ltd., 1998.
- [21] P. Wang et al., Effects of sintering on properties of alumina microfiltration membranes, *J. Membr. Sci.*, 155 (2) (1999) 309–314.
- [22] A. Atkinson and A. Selçuk, Mechanical behaviour of ceramic oxygen ion-conducting membranes, *Solid State Ion.*, 134 (1–2) (2000) 59–66.
- [23] A. Pak, Preparation of zeolite membranes, in Department of Chemical Engineering. 2003, Iran University of Science and Technology: Tehran.
- [24] Y. Zhang, W. Gao and L. Cui, The transformation of acid leached metakaolin to zeolite beta, in Z.G.J.C. Ruren Xu and Y. Wenfu (Eds.), *Studies in Surface Science and Catalysis*, 2007, Elsevier. pp. 420–425.